Iran Red Crescent Med J. 2022 October; 24(10):e1472 doi: 10.32592/ircmj.2022.24.10.1472

Published online 2022 October 20 **Original Article**

Use of Chinese Visible Human Images to Enhance the Interpretation of CT or MRI Images: Application to Nasopharyngeal Structures Segmentation in the Treatment Planning System

Jingyi Yang[1], Xiaoqin Zhang[1], Bangyu Luo[2], Hongjun Liu[1], Zhou Xu[1], Hongkai Wang[3], Xin Hu[1], Jianguo Sun[2], Liang Qiao[4], Shaoxiang Zhang[1] and Yi Wu[1,*]

[1]Institute of Digital Medicine, College of Biomedical Engineering and Medical Imaging, Army Medical University (Third Military Medical University), Chongqing, China
[2]Cancer Institute of the People's Liberation Army, Xinqiao Hospital, Army Medical University (Third Military Medical University), Chongqing, China
[3]Faculty of Electronic Information and Electrical Engineering, Dalian University of Technology, Dalian, China
[4]Department of Medical Image, College of Biomedical Engineering and Medical Imaging, Army Medical University (Third Military Medical University), Chongqing, China

* ***Corresponding author:*** Yi Wu, Institute of Digital Medicine, College of Biomedical Engineering and Medical Imaging, Army Medical University (Third Military Medical University), Gaotanyan Street, Chongqing, China. Tel: 02368771736; Email: wuy1979@tmmu.edu.cn

Received 2021 October 14; **Revised** 2021 November 12; **Accepted** 2022 October 03.

Abstract

Background: With leading morbidity among malignant tumors in otorhinolaryngology, Nasopharyngeal carcinoma (NPC) is one of the most frequent malignant tumors in China.
Objectives: This study aimed to help radiotherapy doctors recognize and segment nasopharyngeal organs at risk of NPC and make a radiotherapy plan.
Methods: The authors used B-spline and mutual information to transform, register, and fuse Chinese Visible Human images with the volunteer's personalized computed tomography (CT) images, and integrated them into the Treatment Planning System (TPS). Consequently, Three-Dimensional Visualization Treatment Planning System (3DV+TPS) was created. To verify it, 3DV+TPS was deployed to identify and segment the nasopharyngeal organs at risk of NPC, and a questionnaire was filled out by radiotherapy doctors.
Results: Results showed that 3DV+TPS can finish the registration and fusion of four sets of sectional anatomical images and individual CT images of volunteers in approximately 3 min and 50 sec.
Conclusion: The registered and fused images can accurately reflect the position, outline, and adjacent space of the nasopharyngeal structure which is not clear in CT images. Therefore, it is helpful for recognizing and segmenting neural, muscular, and glandular structures. Through automatically registering and fusing color and CT gray images, 3DV+TPS improves the accuracy and efficiency of recognizing nasopharyngeal structures in making radiotherapy plans. It is also useful to improve the teaching quality of tumor radiotherapy for medical students and interns as well.

Keywords: B-spline, Image registration fusion, Mutual information, Nasopharyngeal carcinoma, Treatment planning system

1. Background

In China, nasopharyngeal carcinoma (NPC) has become the main cancer and cause of death in otorhinolaryngologic malignancies (1, 2). It is more common in young and middle-aged volunteers in southern China, with a current trend of metastasis to the north (3, 4). The etiology of NPC may be related to genetic, environmental, and Epstein-Barr viral infection factors (5-7). The incidence area is usually the top anterior wall and pharyngeal recess of the nasopharynx (8). The treatment plan for NPC mainly includes radiotherapy, drug therapy, and operation therapy, among which radiotherapy is most commonly used due to its significant effect on improving the survival rate of volunteers and achieving a complete cure (9, 10). However, recognition of the pharyngeal organs at risk in NPC radiotherapies, such as the pharyngeal constrictor, optic chiasm, brainstem, diencephalon, and other neural structures, is very limited due to the low resolution of computed tomography (CT) and magnetic resonance imaging (MRI) grayscale images (11, 12). Especially for junior doctors, it takes much time and energy, and the accuracy of the segmentation is not high.

The Chinese Visible Human dataset has the characteristics of high precision, true color, high resolution, as well as thin layer thickness, and it has a very high recognition ability for the structure of the nasopharynx (13, 14). In this study, the thin-layer high-precision and high-resolution true-color sectional anatomy images (CVH) were deformably registered according to the CT and MRI images of volunteers by B-spline and mutual information and then fused with them and integrated into the TPS radiotherapy system of Xudong Company (Shanghai, China). This technique was attempted by radiotherapy doctors in a clinic to explore and study the practical effects of the registration and fusion method of CVH images, as well as medical images, based on B-spline and mutual information to improve the accuracy and efficiency of radiotherapy doctors in segmenting the target area (15).

2. Objectives

This study aimed to help radiotherapy doctors recognize and segment nasopharyngeal organs at risk of NPC and make a radiotherapy plan.

3. Methods

3.1. Image selection of the structure area of the nasopharynx in the CVH dataset

All materials needed in this experiment were from the intangible and high-precision head and neck sectional anatomical images from the CVH dataset that were frozen and thin-layer-milled in the teaching and research section of the digital medicine of Army Medical University (Chongqing, China), including four cases of CVH1, CVH2, CVH4, and CVH5. The image area was from the top of the head to the lower edge of the thyroid gland. The thickness of the lowest layer of the image was 0.2 mm, the highest image resolution was 4064×2704, and the smallest pixel size was 0.12×0.12 mm. The collection steps of the dataset selected in the experiment were all performed in a low-temperature laboratory below -25°C The milling ice surface did not fog, which made the clarity and accuracy of the dataset image much higher than those of the existing datasets in the world. Moreover, the milling data collected in the low-temperature laboratory could prevent small structures from falling off the milling surface and maintain the integrity of the image data. In addition, the dataset adopted continuous sections of the whole human body without segmental data loss. The main parameters of the dataset selected in this experiment are shown in Table 1.

3.2. CT and MRI image selection of NPC volunteers

The authors selected CT and MRI data of the head and neck of eight volunteers with normal nasopharyngeal structures or early NPC from Southwest and Xinqiao hospitals (Chongqing, China) affiliated with the Army Medical University (Chongqing, China).

The acquisition parameters of CT images included X-Ray tube voltage (100-140kV), X-Ray tube current (28-298mA), image resolution (512×512), pixel size (0.473×0.473 mm), and slice thickness (0.6 mm). The acquisition parameters of MRI images included Repetition Time (715ms), Echo Time (2.6ms), Flip angle (66), Pixel bandwidth (514), resolution (512×512), pixel size (0.553×0.553 mm), and slice thickness (2).

The study was approved by volunteers and their families with informed consent and by the Institutional Review Committee of the Army Medical University. It also followed Chinese ethics and laws.

3.3. Image registration and fusion of the multimodal nasopharyngeal structure based on B-spline and mutual information

Through B-spline and mutual information, CVH head and neck tomograms were registered and fused to CT and MRI images of volunteers to add true-color tomographic anatomy information to the original grayscale images. The method consisted of the following steps: 1) image preprocessing, 2) registration using the spatial transformation model bicubic B-spline surface 3) measuring the degree of similarity between two images in the registration process by mutual information to evaluate the result of image registration, 4) optimizing the problem-solving process by a gradient descent algorithm and searching for the optimal registration parameters that maximize the similarity measure, and 5) matching CVH images with CT and MRI images using the obtained optimal parameters and displaying the fused images (Figure 1).

3.4.1. Integration of CVH nasopharynx data, B-spline, and mutual information algorithm into the TPS software

The CVH color sectional anatomical image and its fused registration image with the CT image were integrated into the 3DV+TPS software from Xudong Company (Shanghai, China). Through this software, radiotherapy doctors can obtain a fused registration image of a color CVH sectional anatomical image with CT and MRI images of volunteers, observe the structure of the nasopharynx, and recognize the anatomical structure of the nasopharynx, which is difficult to recognize on CT and MRI images (Figure 2).

Table 1. Main parameters of the Chinese Visible Human dataset

	CVH-1	CVH-2	CVH-4	CVH-5
Age (y)	35	22	25	25
Gender	male	female	female	female
Height (mm)	1700	1620	1620	1700
Weight (kg)	65	54	57.5	59
Layer thickness (mm)	0.1, 0.5, 1.0	0.25, 0.5	0.25, 0.5, 1.0	0.2
Number of faults	2518	3640	3060	8510
Image resolution	3072×2048	3072×2048	4064×2704	4064×2704
Pixel size (mm)	0.15×0.15	0.15×0.15	0.12×0.12	0.12×0.12

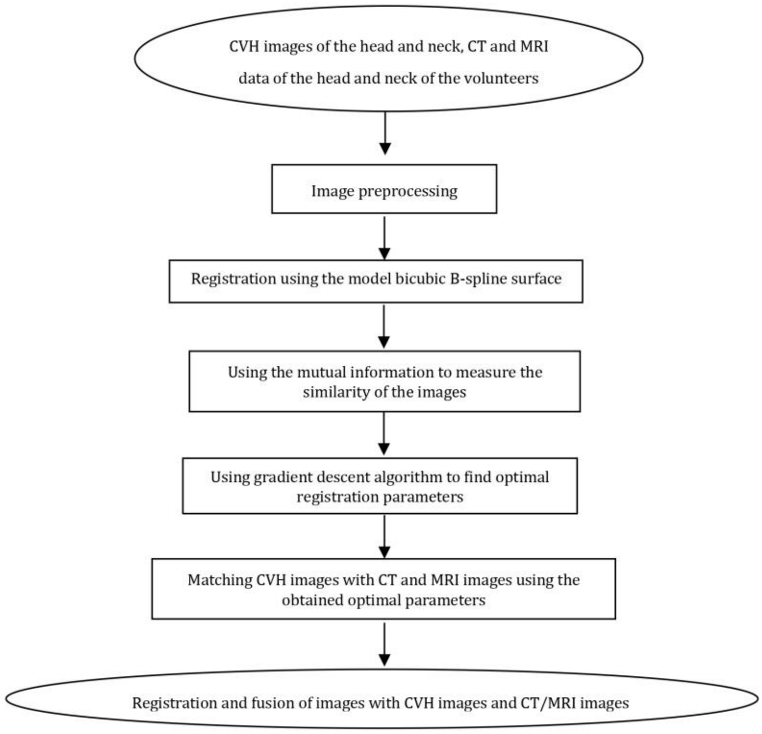

Figure 1. Flowchart of CVH images and CT/MRI images registration fusion method based on B-spline and mutual information
CVH: Chinese Visible Human

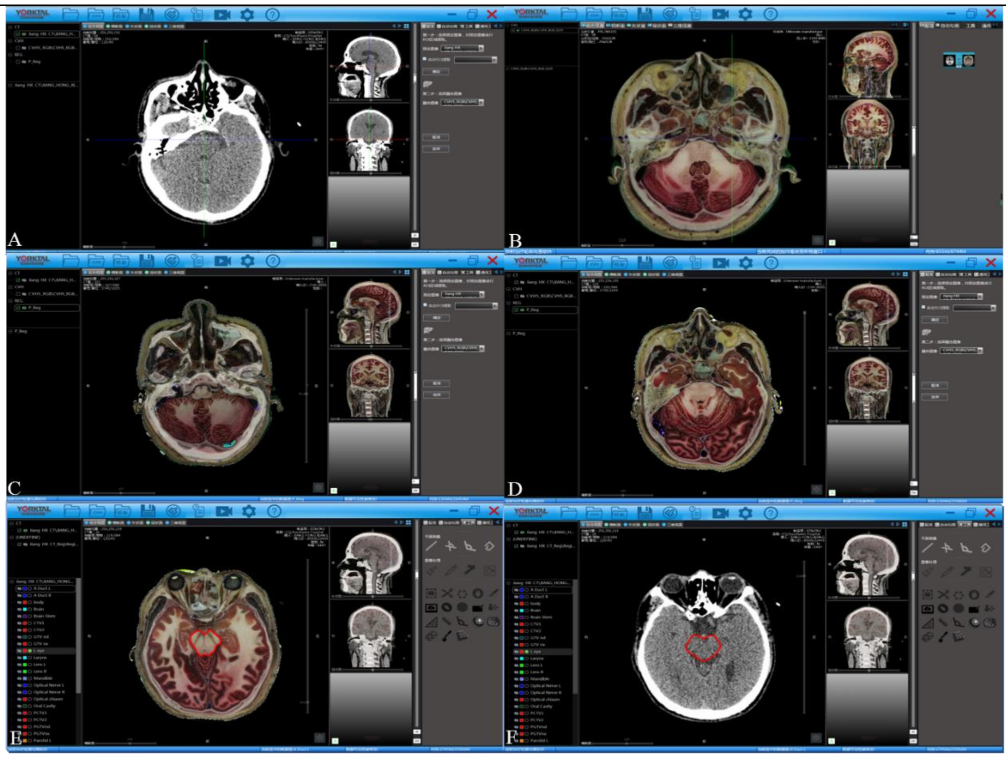

Figure 2. A CVH image is integrated into the 3DV+TPS software after registration and fusion, according to the CT image, and its multimodal image is displayed in the software with 3D visualization

A. The CT image of a volunteer; B. The CVH image of a volunteer; C. Fused registration image of the CVH and CT image of a volunteer; D. The CVH nasopharynx image after deformation based on the CT image; F. Segmentation of the CVH images after the registration fusion of the CVH and CT images; E. The registration fusion of the CT images helping radiotherapy doctors to recognize and segment

3.4.2. Registration and fusion images with CVH and CT/MRI images

Based on the CVH image after registration and fusion, radiotherapy doctors identified and segmented some structures of the nasopharynx on CT/MRI, including the temporal lobe, parotid gland, optic nerve, brainstem, cerebellum, and pharyngeal constrictor.

3.4.3. Selection of CT and MRI images of the same volunteer

The CVH5 image was registered and fused to the cross-sectional MRI and CT images of this volunteer according to the B-spline and mutual information algorithm. The opacity of the deformed CVH image was as the image mask was adjusted. The nasopharyngeal structure in the CVH image and that on the CT image were observed and compared; meanwhile, MRI and CT images were registered and fused for comparison (Figure 3).

3.4.4. Search for the organs at risk of NPC on CVH, CT, and MRI images and comparative analysis by the radiotherapy doctor

A questionnaire (Appendix 1) was designed to evaluate the effect of recognition and segmentation on CVH, CT, and MRI of the organs at risk of NPC. Twenty-two radiotherapy doctors in Xinqiao Hospital (Chongqing, China) completed the questionnaire. Recognition and segmentation effects on the eyeball, lens, brainstem, spinal cord, inner ear, pharyngeal constrictor, parotid gland, temporal lobe, optic nerve, and optic chiasm on CT and CVH images were compared and analyzed. Independent samples t-test was used to investigate the difference between the recognition definition of structures on CT and CVH in CT versus CVH column. (Table 2).

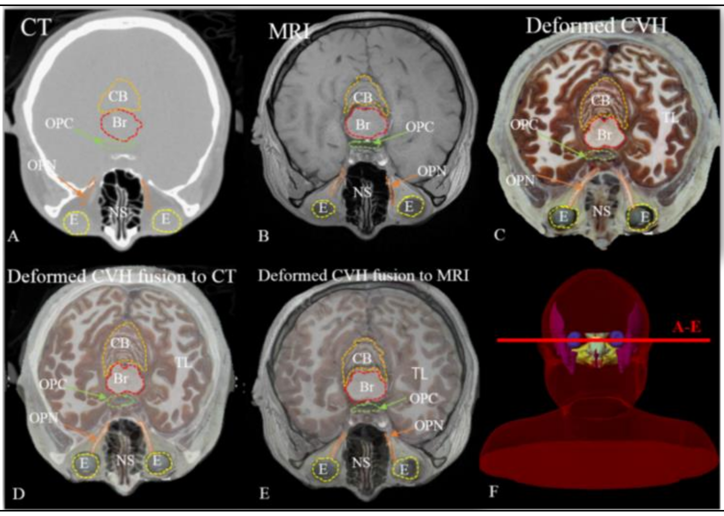

Figure 3. Registered and fused CVH images and MRI and CT images of a volunteer
Br: brainstem; E: eyeball; TL: temporal lobe; OPN: optic nerve; NS: nasal septum; CB: cerebellum; OPC: optic chiasma
A. Volunteer's CT image; B. Volunteer's MRI image; C. Deformed CVH images of a volunteer; D. Registration and fusion of the volunteer's CVH and CT image; E. Registration and fusion of CVH and MRI images; F. A 3D reconstruction of CVH5

Table 2. Comparison and analysis of clarity of CT and CVH recognition structure

Structure	Recognition definition of structure on CT	Recognition definition of structure on CVH	CT versus CVH
Eyeball	4.27±0.88	2.68±1.29	<0.001
Lens	4.32±1.04	2.73±1.29	<0.001
Brainstem	3.45±1.01	3.95±0.72	0.102
Spinal cord	3.73±1.08	3.68±0.84	0.896
Inner ear	2.72±1.08	4.36±0.58	<0.001
Pharyngeal cavity	3.18±1.01	4.22±0.43	<0.001
Pharyngeal constrictor	2.32±1.17	4.27±0.70	<0.001
Parotid gland	2.82±1.29	4.32±0.72	<0.001
Temporal lobe	2.45±1.22	4.41±0.67	<0.001
Optic nerve	3.64±1.05	4.18±0.73	0.09
Optic chiasm	2.00±1.19	4.45±0.74	<0.001

CVH: Chinese Visible Human; Independent samples t-test between recognition definition of structures on CT and CVH was used in CT versus CVH column

4. Results

4.1. Creation of B-spline and mutual information algorithm

A B-spline and mutual information algorithm were created, which achieved the registration and fusion of CVH, CT, and MRI. The image registration and fusion were achieved mainly using image fusion registration of the multimodal nasopharyngeal structure and spatial transformation of the cubic B-spline surface.

4.2. Completion of the registration and fusion of the temporal lobe, parotid gland, and optic chiasm

The temporal lobe, parotid gland, optic chiasm, pharynx muscle (Figure 4), and other structures that could not be recognized on CT/MRI could be identified after integrating the registered and CVH image fused with the CT/MRI images of volunteers into the TPS software (Xudong Shanghai, China), and the fused image could show the corresponding structures clearly.

Several important NPC-endangered organs in radiotherapy, such as the temporal lobe, parotid gland, and optic chiasm, were chosen as representatives for registration, fusion, and structure recognition.

4.3. Design and completion of the questionnaire

There were 22 effectively-responded questionnaires. Of the 22 doctors surveyed, all were doctors or physicians from the Oncology Department of Xinqiao Hospital (Chongqing, China). Eleven of them had only a bachelor's degree, seven had a master's degree, and four had a doctoral degree. The data for each problem was statistically analyzed (Table 2).

According to the findings, the nonrigid registration method of B-spline and mutual information, as well as the registration fusion based on CVH, and the volunteer's personalized CT image could help radiotherapy doctors to identify structures difficult to recognize. It was generally believed that the CVH image was superior to the CT image in identifying the critical structures. The 3DV+TPS could assist radiotherapy doctors in making the operation plan and applying it to clinical operations.

4.4. Statistical verification of the survey questionnaire

The clinicians generally thought that the CVH image was more effective than the CT image in recognizing the organs at risk of NPC (Table 2). Table 2 shows there are differences between CVH and CT/MRI images in the recognition of the eyeball, lens, inner ear, pharyngeal cavity, pharyngeal constrictor, parotid gland, temporal lobe, and optic chiasm. The results also show that CVH images have significant advantages for identifying these structures.

Among the 11 structures surveyed in the questionnaire, the recognition of the eyeball and lens structures was not as good as the CT or MRI images in terms of the enhancement effect of segmentation recognition of the corresponding structures after the registration and fusion of CVH images into CT or MRI images. The enhancement

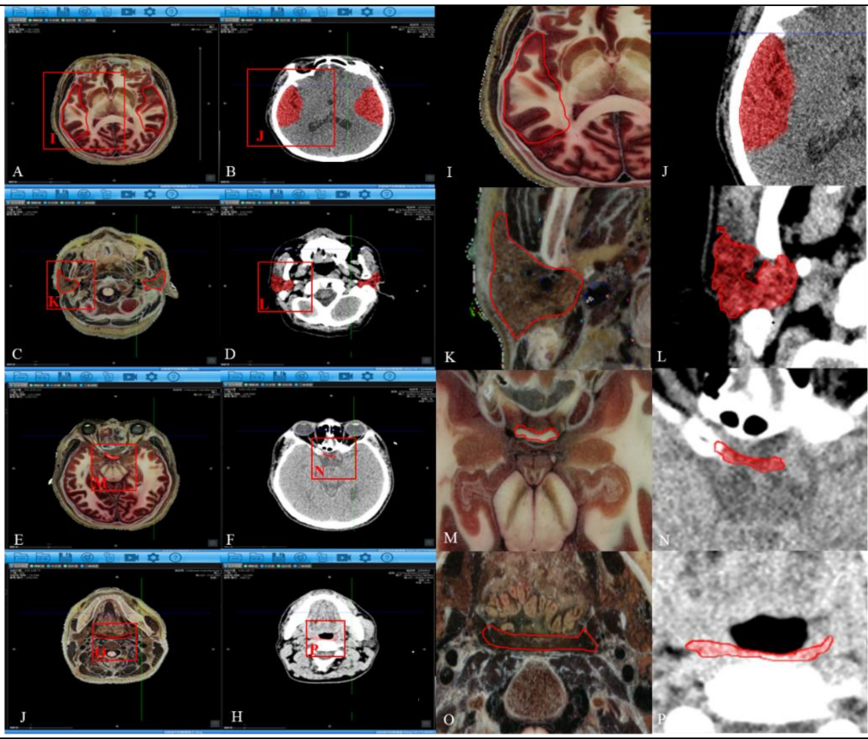

Figure 4. Registration fusion and segmentation of the temporal lobe, parotid gland, optic chiasm, and pharynx muscle
A: The temporal lobe on the CVH image was recognized and segmented after registration. B: The temporal lobe structure on CT could be clearly recognized and segmented through the temporal lobe segmentation of the CVH image. C: The parotid gland was recognized and segmented through the CVH image after deformable registration. D: The parotid gland structure on CT could be clearly recognized and segmented through segmentation of the parotid gland on the CVH image. E: The optic chiasm was recognized and segmented through the CVH image after deformable registration. F: The structure of the optic chiasm on CT could be clearly recognized and segmented through the segmentation of the CVH image. J: The pharynx muscle was recognized and segmented through the CVH image after deformable registration. H: The structure of the pharynx muscle on CT could be clearly recognized and segmented through segmentation of the CVH image. I-P. The numbers i-p are the enlarged corresponding position of the numbers a-h.

effect of the spinal cord, inner ear, pharyngeal cavity, optic nerve, and other structures was quite obvious. On the other hand, the enhancement effect of the brainstem, pharyngeal constrictor, parotid gland, temporal lobe, optic chiasm, and other structures was very obvious. The CVH images can help clinicians complete target area segmentation, successfully deliver precise radiotherapy, and meet the needs of clinical applications.

5. Discussion

In this study, the CVH images were fused with the volunteers' personalized CT and MRI after nonrigid registration based on B-spline and mutual information research methods using a CVH dataset, and the images were integrated into the TPS software. This integration is the first to fuse the true-color and high-precision sectional anatomical images into the radiotherapy contour segmentation process. By this method, radiotherapy doctors can recognize the human body structures that are difficult to recognize on CT images through the sectional anatomical images after deformable registration in the TPS software, such as the brainstem, cerebellum, thalamus, optic nerve, optic chiasm, other nerve tissue structures, the pharyngeal constrictor, other muscle structures, the parotid gland, submandibular gland, and other gland structures. In CT images, the structure of the nerves, muscles, and glands are difficult to recognize and segment precisely due to the close CT value, whereas in the color sectional anatomical images of CVH, the structures of the nasopharynx can be prepared for recognition and segmentation according to their natural colors. Compared to the TPS System of Varian and Medical Kodak (16-19), 3DV+TPS has a unique function in referring to the high-precision true-color anatomical images suitable for an individual volunteer's CT morphology to guide the contour segmentation of organs at risk on CT images more accurately. It is greatly significant for clinicians to accurately segment the target area and organs at risk through radiotherapy, and it can help radiotherapy doctors improve the precision of segmenting at-risk organs, shorten the segmentation time, and improve segmentation efficiency when registered CVH images and CT or MRI images are shown at the same time (17,20). It can help radiotherapy doctors, especially junior ones, make and optimize the radiotherapy plan.

B-spline uses polygons and weight functions to define curves, which can be registered and adjusted for free-form curves and surfaces, while mutual information is used as a similarity measure to evaluate registration results such that registration has a good local deformation effect (21-23). A method of similarity measure based on the unified image grayscale level is proposed to solve the problem where similarity measures based on the grayscale level cannot easily express the relationship between the two images accurately due to the inconsistent grayscale range of images (24,25,26). Therefore, this study is based on the nonrigid registration method of B-spline and mutual information (27). Currently, the authors have constructed eight CVH atlases of different genders, ages, and body weights and will try to match the atlas with the closest head shape to the volunteer to maximize the atlas registration accuracy, which can fit the volunteer's nasopharyngeal structures to a greater extent（28,29）. In this way, the authors hope to further improve the segmentation accuracy of the head structures. In future research, the authors will also consider using multiple CVH atlases to improve the segmentation accuracy.

5.1. Limitations

From the methodological perspective, the present method uses a fully automated registration strategy. However, there are some limitations in this study. First, the automatic method only maximizes the mutual information between the atlas and the volunteer image, which cannot guarantee precise alignment of fine-scale structures, such as nerves and vessels. The reason is that the CVH and NPC volunteers had different bodies and did not match very precisely. Additionally, the 3DV+TPS registration method mainly aims at the integral registration of the local structure of the human body, which cannot meet the personalized accurate registration of a single anatomical structure. Furthermore, the B-spline and mutual information algorithm cannot achieve the manual registration of images (30). The authors' future study will also try to combine the mutual information metric with user intervention of the anatomical landmark definition to allow doctors to control the registration accuracy of local fine-scale structures. Function optimization technology can be used to solve the problem of feature extraction and registration in addition to the transformation of model parameters and optimization of the algorithm to improve the accuracy of automatic registration (31).

6. Conclusion

In this study, four cases of head and neck sectional anatomical images of a CVH dataset were selected, and the CVH image and the volunteer's personalized CT image were automatically registered and fused by the nonrigid registration method of B-spline and mutual information. They were then integrated into the TPS system such that the radiotherapy doctors could identify and segment the organs at risk of NPC based on the CVH color sectional anatomical image. The radiotherapy doctors could accurately identify the position, shape contour, and spatial adjacent relationship of the structure of the nasopharynx on CT images, according to the registration and fusion image of the CVH and the volunteer's individualized CT, and segment them (31). This study is helpful for the recognition and segmentation of the structures that are difficult to recognize on CT images, such as the muscles, nerves, and glands of the nasopharynx. This method achieved the automatic registration and fusion of the color image and CT gray image, improved the accuracy and efficiency of segmentation, is helpful for radiotherapy doctors to make accurate and detailed radiotherapy plans, and helps to improve the teaching quality of tumor radiotherapy for medical students and interns.

Acknowledgments

The authors thank the Xudong Company (Shanghai, China) and Xinqiao Hospital for supporting this study. The authors are also grateful to the doctors who contributed to this questionnaire.

Footnotes

Conflicts of Interest: The authors declare that they have no conflicts of interest.
Authors' Contribution: JY: Data analysis; manuscript writing. XZ: Experiment design. ZX and XH: Provision of materials and literature research. BL and HL: Design and collection of the questionnaire. LQ and HW: Data collection. SZ, JS, and YW: Experiment conception and design.
Funding Statement: The authors are grateful to the National Key Research and Development Project (grant No. 2016YFC0106402), the National Natural Science Foundation of China (grant No. 31671251), the National Natural Science Foundation of China (grant No. 31771324), the Technological Innovation and Application Demonstration of Chongqing CSTC of China (No. cstc2018jscx-msybX0073), and the Graduate Education Teaching Reform Research Project in Army Medical University (No. 2018yjgA009).
Statement of Ethics: The study was approved by the volunteers and their families with informed consent and by the institutional review committee of the Army Medical University (Third Military Medical University).

References

1. Chen W, Zheng R, Zhang S, Zhao P, Li G, Wu L, et al. Report of incidence and mortality in China cancer registries, 2009. *Chin J Cancer Res*. 2013;**25**(1):10-21. doi: 10.3978/j.issn.1000-9604.2012.12.04. [PubMed: 23372337].
2. Wei KR, Zheng RS, Zhang SW, Liang ZH, Li ZM, Chen WQ. Nasopharyngeal carcinoma incidence and mortality in China, 2013. *Chin J Cancer.* 2017;**36**(1):1-8. doi: 10.1186/s40880-017-0257-9. [PubMed: 29122009].
3. Wei KR, Zheng RS, Zhang SW, Liang ZH, Ou ZX, Chen WQ. Nasopharyngeal carcinoma incidence and mortality in china in 2010. *Chin J Cancer*. 2014;**32**(8):381-7. doi: 10.5732/cjc.014.10086. [PubMed: 25096544].
4. Chen WQ, Li H, Sun KX, Zheng RS, Zhang SW, Zeng HM, et al. Report of cancer incidence and mortality in China, 2014. *Zhonghua Zhong Liu Za Zhi.* 2018;**23**;40(1):5-13. doi: 10.3760/cma.j.issn.0253-3766.2018.01.002. [PubMed: 29365411].
5. Chen W, Zheng R, Zeng H, Zhang S, He J. Annual report on status of cancer in China, 2011. *Chin J Cancer Res.* 2015;**27**(1):2-12. doi:10.3978/j.issn.1000-9604.2015.01.06. [PubMed: 25717220].
6. Chang ET, Adami HO. The enigmatic epidemiology of nasopharyngeal carcinoma. *Cancer Epidemiol Biomarkers Prev*. 2006;**15**(10):1765-77. doi:10.1158/1055-9965.EPI-06-0353. [PubMed: 17035381].
7. Lin TM, Chang HJ, Chen CJ, et al. Risk factors for nasopharyngeal carcinoma. *Anticancer Res*. 1986;**6**(4):791-6. [PubMed: 3752958].
8. Huang TR, Zhang SW, Chen WQ, Deng W, Zhang CY, Zhou XJ, et al. Trends in nasopharyngeal carcinoma mortality in china, 1973-2005. *Asian Pac J Cancer Prev.* 2012;**13**(6):2495-502. doi:10.7314/apjcp.2012.13.6.2495. [PubMed: 22938411].
9. Hashemi SM, Mahmoodi R, Amirjamshidi A. Variations in the anatomy of the Willis' circle: A 3-year cross-sectional study from Iran (2006-2009). Are the distributions of variations of circle of Willis different in different populations? Result of an anatomical study and review of literature. *Surg Neuro Int*. 2013;**17**:1-4. doi: 10.4103/2152-7806.112185. [PubMed: 23772335].
10. Trullo R, Petitjean C, Ruan S, Dubray B, Nie D, Shen D. Segmentation of organs at risk in thoracic ct images using a sharpmask architecture and conditional random fields. *Proc IEEE Int Symp Biomed Imaging*. 2017;**2017**:1003-6. doi: 10.1109/ISBI.2017.7950685. [PubMed: 29062466].
11. Han M, Ma J, Li Y, Li M, Song Y, Li Q. Segmentation of organs at risk in CT volumes of head, thorax, abdomen, and pelvis. *SPIE*. 2015;**9413**:942-7. doi: 10.1117/12.2081853.
12. Pradhan S , Patra D . P-spline based nonrigid brain MR image registration using regional mutual information. *India Conference.* 2013;13: 1-5. doi: 10.1109/INDCON.2013.6726145.
13. Zhang SX, PHeng PA, Liu ZJ, Tan LW, Qiu MG, Li QY, et al. Creation of the chinese visible human data set. *Anat Rec B New Anat*. 2003;**275**(1):190-5. doi: 10.1002/ar.b.10035. [PubMed: 14628319].
14. Zhang SX, PHeng PA, Liu ZJ, Tan LW, Qiu MG, Li QY, et al. The chinese visible human (cvh) datasets incorporate technical and imaging advances on earlier digital humans. *J Anat.* 2004;**204**(3):165-73. doi: 10.1111/j.0021-8782.2004.00274.x. [PubMed: 15032906].
15. Sahoo N, Poenisch F, Zhang X, Li Y, Li MF, Li H, et al. 3d treatment planning system—varian eclipse for proton therapy planning. *Med Dosim*. 2018;**43**(2):184-94. doi: 10.1016/j.meddos.2018.03.006. [PubMed: 29753334].
16. Zhao LR, Zhou YB, Li GH, Li QM, Yang DQ, Li HX, et al. The clinical feasibility and performance of an orthogonal x-ray imaging system for image-guided radiotherapy in nasopharyngeal cancer patients: Comparison with cone-beam CT. *Phys Med.* 2016;**32**(1):266-71. doi: 10.1016/j.ejmp.2015.11.010. [PubMed: 26703446].
17. Pradhan S, Patra D. P-spline based nonrigid brain MR image registration using regional mutual information. *IEEE*. 2014. doi: 10.1109/INDCON.2013.6726145.
18. Li HM, Fan Y. Non-Rigid image registration using self-supervised fully convolutional networks without training Data. *Proc IEEE Int Symp Biomed Imaging*. 2018:1-4. doi: 10.48550/arXiv.1801.04012.
19. Zhang S, Liu Z, Liu B, Zhou F. Medical image registration by using salient phase congruency and regional mutual information. In2011 4th International Congress on Image and Signal Processing; 2011.
20. Xiang Y ,Gui P, Wang S. An improved medical image registration method based on the sum of conditional variance. *Biomed Eng Res*. 2018:**37**(1):71-76. doi: 10.19529/j.cnki.1672-6278.2018.01.15.
21. Sahu S, Pati UC. Intensity-based registration of medical images. *Int J Comput Vis Robot.* 2016;**6**(4):319-30. doi:

10.1504/IJCVR.2016.079393
22. Kuruvilla S, Anitha J. Comparison of registered multimodal medical image fusion techniques. Int J Comput Vis Robot. 2014; **13**:1-6. doi: 10.1109/ECS.2014.6892589.
23. Bhattacharya M, Das A. Multimodality medical image registration and fusion techniques using mutual information and genetic algorithm-based approaches. *Adv Exp Med Biol.* 2011;**696**:441-9. doi: 10.1007/978-1-4419-7046-6_44. [PubMed: 21431584].
24. Sobottka SB, Steinmeier R, Beuthien-Baumann B, Mucha D, Schackert G. Evaluation of automatic multimodality fusion technique of PET and MRI/CT images for computer assisted brain tumor surgery. *Int Congr Ser.* 2001; 1230(1): 261-267. doi: 10.1016/S0531-5131(01)00053-X.
25. Yin F, Gao W, Song Z. Medical image fusion based on feature extraction and sparse representation. *Int J Biomed Imaging.* 2017;**2017**:1-11. doi: 10.1155/2017/3020461. [PubMed: 28321246].
26. Liu Z, Yin H, Chai Y, Yang SX. A novel approach for multimodal medical image fusion. *Expert Syst Appl.* 2014;**41**(16):7425-35. doi:10.1016/j.eswa.2014.05.043.
27. Mirzadeh Z, Chapple K, Lambert M, Dhall R, Ponce FA. Validation of CT-MRI fusion for intraoperative assessment of stereotactic accuracy in DBS surgery. *Mov Disord.* 2014;**29**(14):1788-95. doi: 10.1002/mds.26056. [PubMed: 25377213].
28. Yang R, Li QX, Mao C, Peng X, Wang Y, Guo YX, et al. Multimodal image fusion technology for diagnosis and treatment of the skull base-infratemporal tumors. *Beijing Da Xue Xue Bao Yi Xue Ban.* 2019;**51**(1):53-8. doi: 10.19723/j.issn.1671-167X.2019.01.010. [PubMed: 30773544].
29. Chuang WY, Chang SH, Yu WH, Yang CK, Yeh CJ, Ueng SH, et al. Successful identification of nasopharyngeal carcinoma in nasopharyngeal biopsies using deep learning. *Cancers (Basel).* 2020;**12**(2):1-11. doi: 10.3390/cancers12020507. [PubMed: 32098314].
30. Klein S, Staring M, Pluim JP. Evaluation of optimization methods for nonrigid medical image registration using mutual information and b-splines. *IEEE Trans Image Process.* 2007;**16**(12):2879-90. doi: 10.1109/tip.2007.909412. [PubMed: 18092588].
31. Rueckert D, Aljabar P. Non-rigid registration using free-form deformations. Handbook of Biomedical Imaging. Boston: Springer; 2015.

Appendix 1

Questionnaire on the effect of the CVH deformable model in radiotherapy

This questionnaire was specially formulated to understand the practical application effect and satisfaction of the CVH deformable model in clinical radiotherapy more comprehensively. It is expected to provide the basis for the subsequent improvement in the model through investigation and finally meet the needs of clinical radiotherapy to a greater extent.

1. Questionnaire Description:
(1) This questionnaire is concise and easy to answer.
(2) You can fill in this questionnaire anonymously. The letters involved in this questionnaire will be strictly confidential, so you can answer with confidence.
(3) Please answer according to the actual situation; otherwise, it may affect the accuracy of the survey results.
2. Background information: Please tick "√" in front of the corresponding item according to the actual situation.

Radiotherapy center	**Xinqiao Hospital**	**Date of filling**	**Y M D**
Title		**Gender**	□**Male** □**Female**
Age	□Under 25 years □26-35 years □36-45 years □Above 46 years		
Education	□Junior College □Undergraduate □Master's □Doctor		
Department	□Oncology □Radiology □Surgery □Internal medicine		

3. Select the most appropriate answer by ticking "√"

Delineating/identifying parts (not completely and clearly delineated on CT)	**Very clear (5 points)**	**Clear (4 points)**	**Uncertain (3 points)**	**Unclear (2 points)**	**Very unclear (1 point)**
Eyeball	A	B	C	D	E
Lens	A	B	C	D	E
Brainstem	A	B	C	D	E
Spinal cord	A	B	C	D	E
Inner ear	A	B	C	D	E
Pharyngeal cavity	A	B	C	D	E
Pharyngeal constrictor	A	B	C	D	E
Parotid gland	A	B	C	D	E
Temporal lobe	A	B	C	D	E
Optic nerve	A	B	C	D	E
Optic chiasm	A	B	C	D	E

Parts with an improved delineation effect of the threatened organ in the head and neck in radiotherapy after CVH image registration and fusion	**Very obvious (5 points)**	**Obvious (4 points)**	**Uncertain (3 points)**	**Unobvious (2 points)**	**Very unobvious (1 point)**
Eyeball	A	B	C	D	E
Lens	A	B	C	D	E
Brainstem	A	B	C	D	E
Spinal cord	A	B	C	D	E
Inner ear	A	B	C	D	E
Pharyngeal cavity	A	B	C	D	E
Pharyngeal constrictor	A	B	C	D	E
Parotid gland	A	B	C	D	E
Temporal lobe	A	B	C	D	E
Optic nerve	A	B	C	D	E
Optic chiasm	A	B	C	D	E

In addition, what are your personal needs for radiotherapy? Or what are your opinions or suggestions regarding the existing model?